Langmuir

Article

pubs.acs.org/Langmuir

Temperature-Induced Collapse, and Arrested Collapse, of Anisotropic Endoskeleton Droplets

Marco Caggioni,[†] Jessica Lenis,[†] Alexandra V. Bayles,[‡] Eric M. Furst,[‡] and Patrick T. Spicer*[,§]

[†]Microstructured Fluids Research, Procter & Gamble Co., Cincinnati, Ohio 45202, United States

[‡]Department of Chemical and Biomolecular Engineering and Center for Molecular and Engineering Thermodynamics, University of Delaware, Newark, Delaware 19716, United States

[§]School of Chemical Engineering, UNSW Australia, Sydney, NSW 2052, Australia

ABSTRACT: Micron-scale rod-shaped droplets with a range of aspect ratios are produced using extrusion of oil containing a soft wax crystal network to permit shape customization. A physical model of the droplet shape stability is developed based on balancing interfacial stresses with the internal crystal network yield stress. The model predicts the mechanical properties required for particular droplet size stability, in a given physicochemical environment, and is tested by microscopic observations of droplets over a range of relevant applied temperatures. The time-dependent response to temperature of individual rods is monitored and used to identify the collapse temperature based on structural yielding. Precise temperature control allows variation of the droplet endoskeleton yield stress and direct determination of the droplet stability as a function of size, by observing the onset of collapse by interfacial compression, and enables validation of the model predictions. Mapping the regions of droplet stability and instability for various-sized droplets yields a basis for designing droplet shapes for multiple applications using easily measured physical variables. The phenomenon of arrested collapse is also explored as a means of transforming simple rod-shaped starting materials into more complex shapes and enhancing adhesion to targeted solid surfaces, enabling exploitation of the hybrid solid−liquid nature of these droplets.

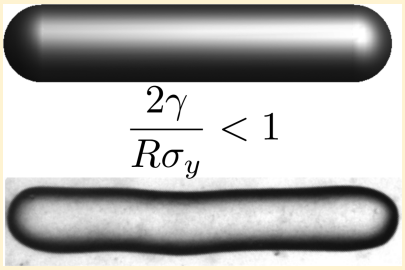

INTRODUCTION

The delivery of dispersed materials from a flowing liquid or gas stream to a targeted surface is a widely used technique in foods, cosmetics, pesticides, and pharmaceuticals. Although particle size is a key variable, affecting inertial deposition,[1] particle shape has recently been found to have a profound impact as well. For example, injected polymer particles with elongated shapes are known to limit phagocytosis by macrophages and enable controlled uptake,[2,3] while the shape and density of aerosolized particles control their delivery in the lung.[3−6] Shape ultimately expands the utility of dispersed particles by improving retention in porous materials,[7] adding directional control to particle trajectories,[5,8] and enabling specificity of interactions with other surfaces via lock and key dynamics.[9]

The shape of liquid droplets is typically restricted to spheres as a result of the interfacial tension that minimizes the surface free energy. As a result, emulsion systems are mostly unable to adopt stable anisotropic shapes and enable the same benefits provided by solid nonspherical colloids in a dispersion. However, emulsions are a common basis for vaccine, aerosol, cosmetic, and pesticide formulations because of their ability to dissolve and stabilize a wide range of biological and chemical active ingredients. A broader ability to create shaped liquid droplets would expand the control, impact, and efficiency of emulsion formulations by reapplying the benefits of anisotropic solid colloids while retaining the ability of droplets to dissolve actives and wet targeted surfaces. Shaped droplets have been produced before, though past work has used either permanent shaping via solidification,[10−12] adsorption of structured monolayers,[13−20] contact with solid surfaces,[21−23] or temporary methods like external fields[24] to stabilize anisotropic shapes, limiting their respective wetting and long-term stability. We emphasize here that this work focuses on freely dispersed anisotropic droplets that require only an internal yield stress to hold their shape.

Previous work on arrested structures formed during colloid synthesis[25] and emulsion droplet coalescence[26,27] offers a conceptual basis for producing shaped droplets by balancing interfacial pressures, driving a droplet toward sphericity, with rheological forces that can stably resist such deformation.[28] The resulting viscoelastic droplets possess a hybrid structure that can be shaped into numerous anisotropic shapes because of an internal elastic network of solids but still behave externally as a liquid droplet by wetting and adhering to compatible surfaces. Such droplets can take on a wide range of shapes, like a solid colloid, while retaining the liquid surface and dissolution properties of a droplet. A key concept here is the dynamic balance achieved between interfacial and rheological forces that can be used to stabilize a desired shape and then optionally trigger a change to a more complex or compact form by simply adjusting the magnitude of the droplet yield stress. A physical model of the droplet shape stability has been previously

Received: January 27, 2015
Revised: June 29, 2015
Published: July 15, 2015

DOI: 10.1021/acs.langmuir.5b00321
Langmuir 2015, 31, 8558−8565

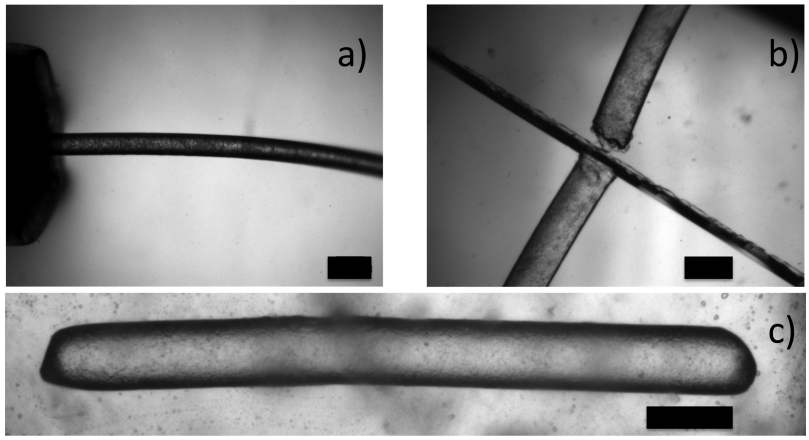

Figure 1. Micrographs of the extrusion process used to make endoskeleton droplets, here containing 70% petrolatum. Scale bar is 300 μm. In (a) the droplet exits the tube after being shaped and the random network of anisotropic crystals making up the internal droplet microstructure provides stability against collapse into a sphere. The rod extrudate is then cut to desired length in (b) to suit a specific use, although a microfluidic realization of this process is also conceivable.[12] A close-up view of a typical rod produced by this method is seen in (c), where the curved ends of the rod emphasize the liquid character of its surface.

developed to describe the balance of interfacial and rheological forces acting on shaped droplets.[28] The model accurately predicts collapse of elongated droplets into more compact shapes when the interfacial force is suddenly raised via dilution.[28] Here, the model's description of rheological force variations is studied, through microscopic observations of rod-shaped droplet shape change and collapse, during temperature-induced reduction of the internal network yield stress. The resulting map of stability provides a design guide for droplets with stable size and shape for a particular application, or chemical environment, as well as tunable shape-change response to external triggers like temperature.

EXPERIMENTAL SECTION

Rod-shaped endoskeleton droplets are made of a mixture of hexadecane (99%, Sigma-Aldrich) and petrolatum (Unilever, 50% w/w solids) that provides an internal skeleton of wax crystals with an average aspect ratio of 100.[27] Although surface-active species can cause crystals to partition at droplet interfaces, or cross them entirely,[29] for this system we see no visual evidence, within the 0.3 μm resolution of our microscopes, of interfacial adsorption of any crystals at the oil–water interface. The droplets are produced by extrusion using a syringe pump (Harvard Apparatus) from a heated metal syringe (New Era Pump Systems) through tubing (IDEX FEP), with a range of internal diameters between 60 and 250 μm, connected to its outlet, and then cut to length (Figure 1). Heating tape (Omega) is wrapped around the syringe and set to a temperature of ∼61 °C to keep the mixture fluid in the syringe, but the outlet tube length is sufficient to allow the mixture to cool and mostly solidify. Plug flow in the tubing does not significantly disturb the internal microstructure near the exit. The extruded material is collected in a container of a 10 mM solution of sodium dodecyl sulfate (Fluka) in water weakly structured with 0.5% w/w microfibrous cellulose (CP-Kelco). Once rods are made to a desired size and shape, they are transferred to a microscope cell in a Linkham THMS 600 controlled temperature stage on a Zeiss Axioplan 2 microscope where their shape evolution is studied as temperature is changed. The study of individual droplets is made easier by the small yield stress imparted by the cellulose.

The bulk yield stress of the droplet phase is measured in the linear viscoelastic regime by oscillatory experiments using a TA Instruments AR2000 rheometer in strain-controlled mode at a frequency of 1 Hz as the elastic modulus exhibits no frequency dependence between 0.01 and 1 Hz. The critical strain is determined to be the point at which the elastic modulus drops rapidly, and the yield stress is calculated as the product of the plateau modulus and the critical strain. Separate measurements are performed on different samples for each temperature.

For the hexadecane–petrolatum dispersion studied here, the anisotropic colloidal network in the droplets is highly thixotropic, and the oscillatory measurement is used to avoid any bias induced by previous shearing or by aging. The oscillatory sweep explores from small to large deformations, from small-amplitude oscillatory strain to large-amplitude oscillatory strain, enabling us to determine the transition from linearity to nonlinearity as the microstructure yields. However, the bulk measurements are performed using a tool with a much larger length scale than the wax crystals making up the elastic network, while the droplets are much closer to the actual size of the crystals, and the droplet-scale deformation during collapse may be quite different from that determined by a bulk measurement. Droplet interfacial tension is measured using a Kruss DSA100 pendant drop tensiometer.

RESULTS AND DISCUSSION

The production of droplets by extrusion in Figure 1 indicates the droplet's solid-like ability to retain a deformed shape, as it would rapidly collapse to a sphere without the yield stress imparted by the endoskeleton structure. For sufficiently strong endoskeletons, the shape is preserved and stable rods of length-to diameter aspect ratios, AR, as large as 30 can be produced. The extrusion method enables the production of a wider range of droplet radius and length, in a shorter time, than our previous molding method,[27] enabling more detailed study of the rod shape stability. The yield stress of the material comprising the rods varies strongly as a function of temperature, losing all elasticity above 50 °C and becoming an easily handled Newtonian fluid at higher temperatures. When cooled, however, the mixture rapidly increases in viscosity and elasticity as solid wax particles crystallize out of solution in the oil. The droplet oil phase solid content is zero at high temperature because of mutual solubility and at room temperature can be varied between 0% and 50% depending on the petrolatum–hexadecane ratio used. While at fixed temperature the solid fraction is determined by the petrolatum–hexadecane ratio, the droplet solid content varies in the range of 25–55 °C because of the breadth of the wax crystal melting point distribution. The spread of melting points allows us to tune the solid content of a single sample, and its yield stress, by varying the temperature. The inset in Figure 2 demonstrates the determination of

DOI: 10.1021/acs.langmuir.5b00321
Langmuir 2015, 31, 8558–8565

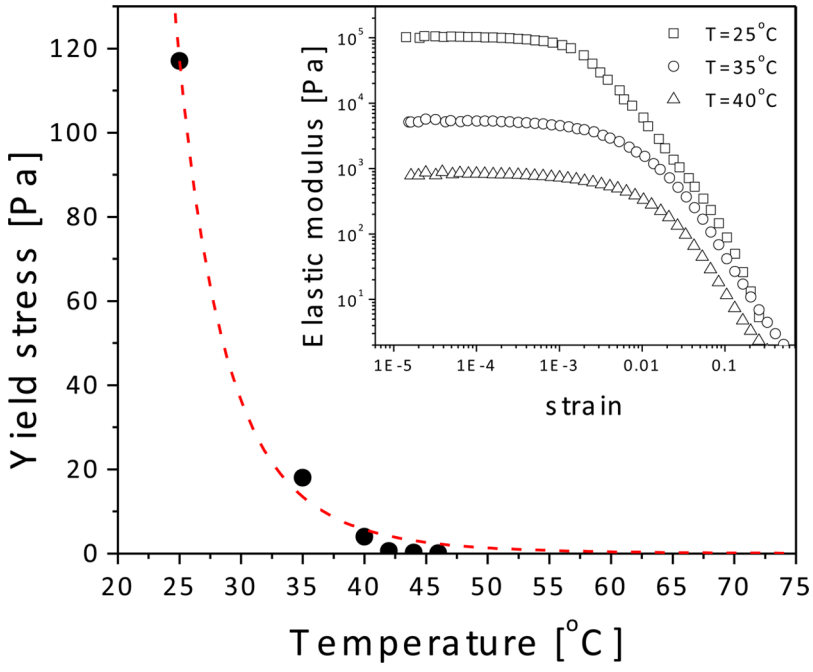

Figure 2. Deformation of droplets is preserved using an elastic network of wax crystals that is completely wetted by the droplet fluid. As for all concentrations studied, the elasticity of a mixture of 70% petrolatum and 30% hexadecane declines at temperatures above ambient. Yield stress decreases more rapidly with increased temperature, but the polydispersity of the crystals still provides a broad range of variation. The dashed line is a simple fit to guide the eye.

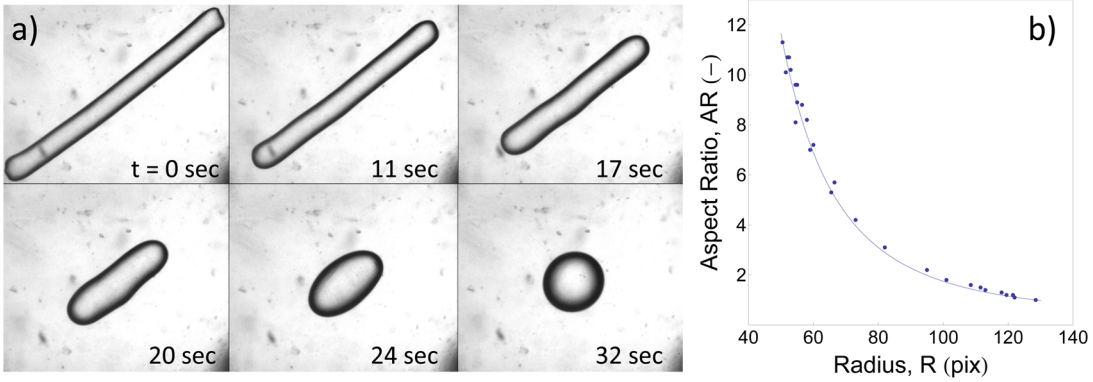

Figure 3. Collapse of a rod back to a sphere occurs upon heating at ~20 °C/min in (a) while good agreement between the geometric model (solid line) of eq 1 and the experimentally determined values of aspect ratio and end-cap radius is found in (b), indicating nearly ideal intermediate states and rapid equilibration at each temperature.

droplet yield stress via an oscillatory strain sweep. The dispersion has a strain-independent elastic modulus, G', at low strains and yields above a critical strain when the original elastic properties are lost. We use the oscillatory data to determine the yield stress for each temperature as the solids content decreases.

The ability to tune the droplet yield stress enables studying, controlling, and applying the collapse of a shaped droplet. The most idealized form of collapse involves instantaneous removal of the skeleton, allowing interfacial tension to act unimpeded, minimize the surface energy, and return the spherocylinder shape to a sphere. Such a case may be experimentally approximated by quickly heating and melting the droplet endoskeleton. Figure 3a shows the collapse of an initially stable spherocylinder droplet with an aspect ratio of ~11 while heating at ~20 °C/min up to ~60°C, where we expect no solid crystals to be present based on Figure 2. The collapse sequence in Figure 3a follows a surprisingly ideal progression of shapes as the droplet returns to sphericity, indicating rapid equilibration of the interface throughout the fast-heating process.

A prediction of the calculated droplet dimensions in Figure 3b is made by determining the aspect ratio, AR, of a spherocylinder with constant volume, V, as a function of its end-cap radius, r, using

$$\mathrm{AR} = \frac{V}{2\pi r^3} + \frac{1}{3} \tag{1}$$

The experimental values of aspect ratio and radius are determined from image analysis of a bounding rectangle's dimensions at each step of the collapse. The droplet volume is assumed constant and determined using the spherical dimensions in the final frame of the image series. The excellent agreement between theory and experiment in Figure 3b, as well as with theoretical work on droplet elongation,[30] indicates the

DOI: 10.1021/acs.langmuir.5b00321
Langmuir 2015, 31, 8558−8565

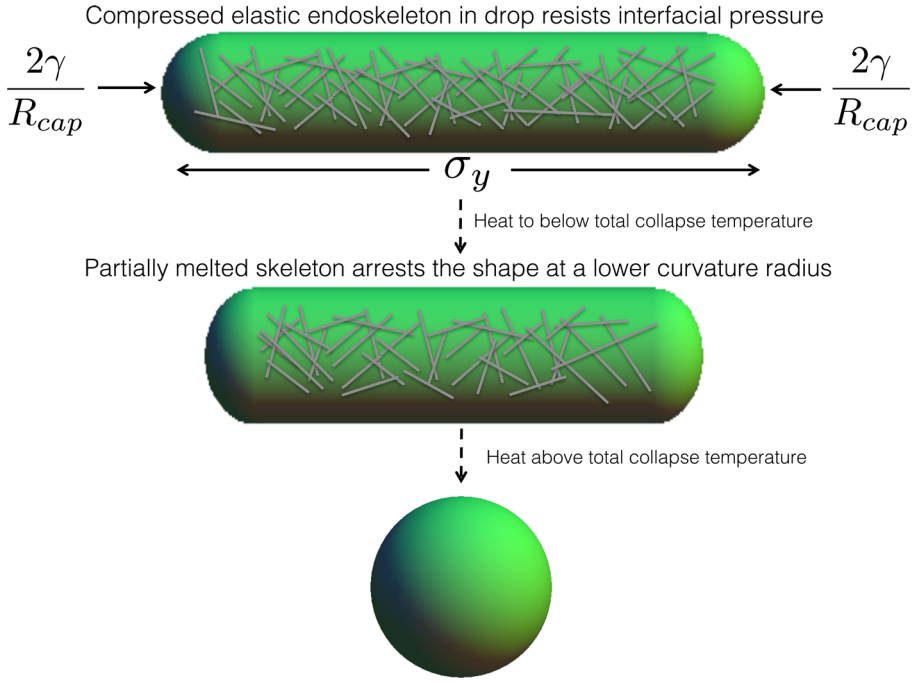

Figure 4. Droplet stability is modeled assuming a spherocylindrical shape and a compressive stress by the Laplace pressure that opposes the internal network elasticity. Shifting this balance of forces, for example by partially melting the endoskeleton and reducing the rod yield stress, can cause linear elastic deformation of the rod and adjustment to a shorter rod shape. Heating above the collapse temperature causes total failure of the endoskeleton and collapse of the rod into a spherical droplet.

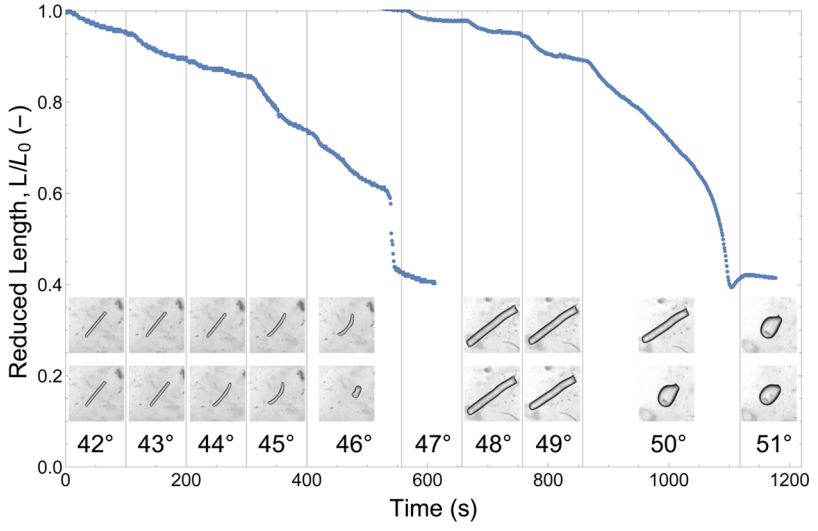

Figure 5. An example of the data used to determine rod collapse temperature is shown for two rods with 100% petrolatum, and a similar aspect ratio, but different end-cap radii. The dimensionless length of the rods is slowly reduced by heating, to lower the internal yield stress, and collapse occurs at a higher temperature for the larger end-cap radius rod (75 μm, right-hand data) as a result of the lower Laplace pressure on that shape. Snapshots of the droplet at the beginning, top row, and end, bottom row, of each temperature step are shown to explain the nature of the deformation observed.

loss of all significant endoskeleton solids at a rate faster than drop shape relaxation occurs. Equation 1 enables prediction of collapse dynamics and intermediate shapes when heating is rapid. Comparison of the first and last images also emphasizes the significant difference in characteristic dimension of the droplet between its elongated and compact forms. Such shape variation permits the same volume of liquid, deformed via stable elongation, to offer a much larger collision profile to a target in a flow. Application of the stabilization and collapse of endoskeleton droplets, especially in a controlled fashion, requires a physical model that explains both and maps the limits of the behavior observed so far.

Applying a theoretical model proposed to explain arrested coalescence of spherical structured droplets,[27] and previously used to model interfacially induced collapse of molded shaped droplets,[28] we propose here that the ability of these droplets to maintain anisotropic shapes is explained by a simple balance between interfacial and elastic forces. For a droplet with internal microstructure, stress is applied by the droplet interfacial tension on the internal elastic structure, deforming it and producing an elastic reaction. For sufficiently strong

DOI: 10.1021/acs.langmuir.5b00321
Langmuir 2015, 31, 8558−8565

elastic structures, the interfacial pressure is offset, and stable anisotropic shapes are obtained. By generalizing this model, we expect that elastic endoskeletons, inside emulsion droplets distorted into anisotropic shapes, always experience a compressive stress not offset by the incompressible droplet liquid phase. For an idealized spherocylindrical droplet (Figure 4), the compressive stress, σ_i, due to the interfacial tension, γ, should be of the order of the Laplace pressure applied by the two hemispherical caps, with radius R_{cap}, on the cylindrical section:

$$\sigma_i = \frac{2\gamma}{R_{cap}} \tag{2}$$

In the absence of a sufficiently high yield stress, the structure yields and the droplet relaxes toward a more isotropic shape. The critical minimum cap radius R_{cap}^{min} is then a function of σ_y and γ:

$$R_{cap}^{min} = \frac{2\gamma}{\sigma_y} \tag{3}$$

so that with a constant interfacial tension, γ, the rod yield stress, σ_y, and maximum surface curvature, $1/R_{cap}^{min}$, rather than aspect ratio, determine rod stability. An interesting prediction of this simplified model is that rod length does not affect shape stability, provided interfacial tension and rod radius are appropriate for a given endoskeleton's mechanical properties. The extrusion process used here allows the production of rods with very large aspect ratios by dispersing or cutting to a desired length.

In order to evaluate the physical model, we study the onset of endoskeleton droplet collapse during slow heating. Droplets are observed while being held at a constant temperature for at least 100 s until it is clear that true collapse has not begun. Collapse does not occur until a critical temperature is reached, and the elastic microstructure is sufficiently weak to yield to the constant interfacial forces. It is therefore possible to systematically vary the droplet yield stress, and shift between stability and collapse, by heating the droplet and gradually melting its endoskeleton. Collapse onset is determined to be the temperature where significant and irreversible rod deformation occurs. The evolution of two endoskeleton droplets with temperaure and time is shown in Figure 5. The dimensionless length of the droplet shows the kinetic and elastic response of the rod to the constant Laplace pressure exerted by the interface as increased temperature lowers the yield stress. The interfacial pressure remains constant throughout the experiment, but the stepped increase in temperature lowers the rod yield stress by incrementally melting away the endoskeleton components. This can be seen by the slight decrease in length, ~5%, at each new temperature, reflecting small linear elastic deformations of the rod as a new, lower, elastic modulus forces the rod to equilibrate at a smaller length. Both rods follow this pattern for the early stages of their heating and at a similar rate. The next stage of deformation is a partial bending of each rod, as seen by the inset images for the left-hand, smaller rod shape in Figure 5 for the 45 °C temperature zone. We do not consider the initial bending to be true collapse but more of a plastic deformation, or buckling, of the rod. A similar partial collapse occurs for the larger, right-hand rod at 50 °C. The two rods differ in their end-cap radius, but this is enough to cause a four degree difference in collapse temperatures, with the smaller radius rod yielding earlier as a result of the higher Laplace pressures. We perform these measurements for a range of droplet radii and solids concentrations and find a similar progression for all three concentrations: higher radius rods experience a smaller compression force and thus yield at a higher temperature.

Figure 6 summarizes the data obtained from plots like Figure 5 and shows the variation of collapse onset temperature as a function of both rod radius, which determines the magnitude of interfacial pressure (eq 2), and solids concentration, which determines the yield stress. For all concentrations, increasing droplet radius reduces the compressive tension on the droplet and increases the collapse onset temperature. For a constant radius, greater solids content increases the temperature of collapse by as much as ~20 °C. The data in Figure 6 are gathered using rods with a wide range of aspect ratios, from 2 to 40, and this, as well as the similar shape of the curves in Figure 6, indicates the apparently universal applicability of eq 3. Toward this end, the data in Figure 6 can be used to convert from collapse temperature to instantaneous yield stress using the yield stress data in Figure 2. Plotting the data for several solids concentrations and rod dimensions enables comparison of eq 3 with experimental observations and produces reasonable agreement without fitting in Figure 7. The solid line in Figure 7 plots eq 3 using the measured interfacial tension, $\gamma \sim 1.5$ mN/m. The emulsion has a relatively low interfacial tension because of the surface active materials accompanying the endoskeleton waxes and the aqueous surfactant present.[27] Although eq 3 is a basic physical model, we are encouraged by its successful prediction of the general collapse of the data in Figure 7. Although agreement is relatively good between data and model, given that no fitting is performed, more studies will be needed to understand the limits of this behavior at lower end-cap radii than we have been able to study here.

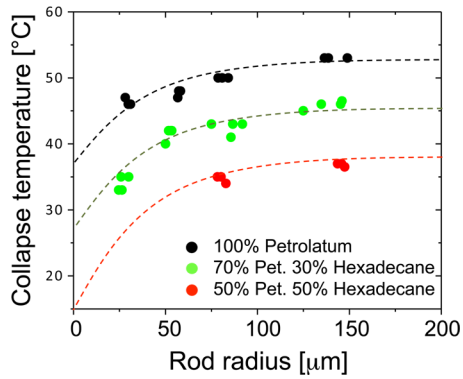

Figure 6. Plotting the onset temperature of collapse, during slow heating, as a function of rod radius and solids level shows the ability to control triggered collapse by tuning mechanical properties via compositional adjustments.

Beyond retention of stable, nonspherical droplet shapes, controlling collapse via arrest is also of interest because it enables a change of shape, over a number of possible intermediates between a rod and sphere, by applying different heating rates. Figure 8 shows three time-lapse sequences of rods collapsing by different modes as they are heated. Because the wax crystals comprising the endoskeleton have a broad distribution of melting temperatures, and are distributed throughout the rod volume, it is possible for onset of collapse, or a buckling instability, to occur at multiple locations in a given

DOI: 10.1021/acs.langmuir.5b00321
Langmuir 2015, 31, 8558−8565

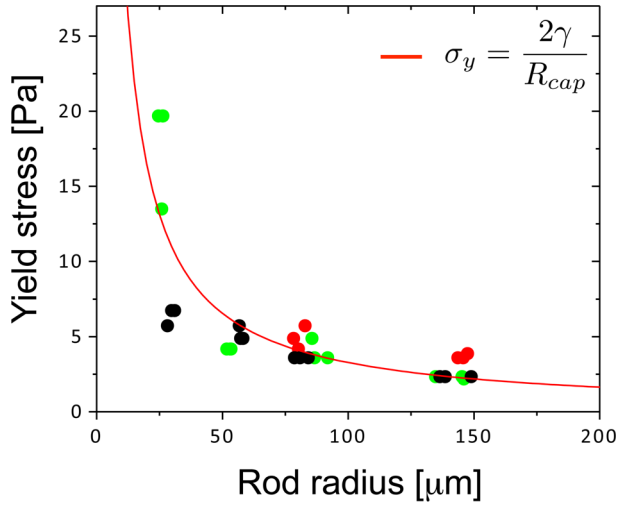

Figure 7. Solid line, eq 3, exhibits good agreement with experimental data for multiple compositions and droplet end-cap radii, and the general collapse of the experimental data indicates that the key physical variables affecting collapse are captured.

rod. As a result, numerous variations of collapse are possible, offering additional applications for these structures. When failure occurs near each end of the rod, as in Figure 8a, simultaneous rolling toward the rod center occurs. A double failure nearer the rod center leads to a shearing motion around the joints of a three-part endoskeleton, resulting in a z-shaped endoskeleton inside the droplet in Figure 8b. A more distributed failure of the rod in Figure 8c drives a curling motion that results in a droplet containing a ring-shaped endoskeleton. As the droplet collapses, its end-cap curvature continuously decreases, as does the corresponding Laplace pressure. It is therefore not surprising that stable intermediate structures are often reached before a compact sphere is formed. Such arrested collapse offers an opportunity to produce many new shapes, all from the same starting point, simply by melting. The resulting, more complex, shapes can then be preserved by returning to a lower temperature to resolidify the endoskeleton before melting is complete.

Another fascinating form of collapse is a directed rolling that can occur when failure near one end of a rod-shaped droplet initiates collapse. The rod in Figure 9 begins rolling once it has been slowly heated, at 0.5 °C/min, to 43 °C, well below the temperature of 57 °C required to liquefy a 70% petrolatum mixture (Figure 6). Once begun, rolling proceeds linearly along the rod axis until the entire endoskeleton has been deformed into a spiral, or cinnamon roll, shape. Cooling back down to 25 °C then solidifies the structure, allowing verification of its two-dimensional disk-like nature by micromanipulation. We term this intermediate state arrested collapse, and it offers an approach to forming more complex shapes from an initially anisotropic droplet. The arrest region exists between total collapse, when the drop endoskeleton is completely melted, and the onset of collapse. Arrested collapse is thus a means of directed formation of new, more complex or useful shapes than even the starting rod shape.

Although unique shapes can be formed by rod collapse, guided only by interactions with the external fluid, other biasing of the collapse process can further expand the range of shapes produced. As the Laplace pressure exerted by the external fluid drives uniaxial collapse in our simple model, the addition of an off-axis directional force can alter the path taken during collapse and the resulting shape. Prior to triggering collapse, contacting a rod with a wetted shape like an air bubble creates a gradient in the Laplace pressure between the end-cap radius and the meniscus between the droplet and bubble, as in Figure 10a. Once collapse begins, the droplet is pulled by the bubble-droplet meniscus, and its opposite sign curvature, around the bubble's perfectly spherical surface until it meets its other end, creating the ring shape shown in the final frame of Figure 10a. As in Figure 9, the resulting shape is then arrested by cooling to resolidify.

In addition to a foundation for synthesis of more complex droplet shapes, the rod-shaped droplet offers significant potential for enhanced deposition, and retention, of droplet-based delivery vehicles. Elongating a spherical droplet into a rod enhances its collision profile by a significant factor, assuming high rotational mobility. Once a droplet delivery vehicle is deposited on a surface of interest, retention is desirable but can be low if fluid flow continues around the targeted substrate. Triggering collapse by heating, after deposition occurs, drives an additional form of shape change that leads to the droplet curling itself helically around the surfaces, as seen for the case of a cylindrical fiber in Figure 10b. While here the contact area of the droplet on the substrate is constant before and after collapse, the new orientation provides an additional element favoring retention in a flow as the droplet's point of attachment is no longer unidirectional. Collapse of shaped droplets shows the potential to create a

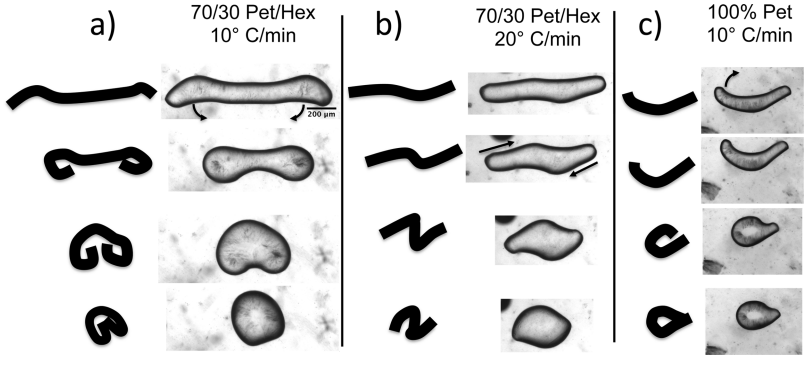

Figure 8. Variability of collapse mode for initially rod-shaped droplets depends on the number and location of points of initial structural failure. To the left of each example is a schematic tracing of the droplet skeleton at each stage of collapse to emphasize the possible grasping, shearing, and folding modes observed.

DOI: 10.1021/acs.langmuir.5b00321
Langmuir 2015, 31, 8558−8565

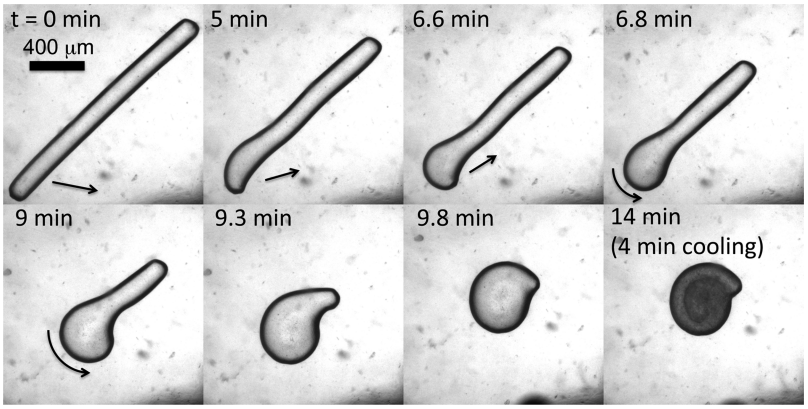

Figure 9. At slower heating rates, ~0.5 °C/min, unidirectional rolling produces a number of interesting intermediate structures in a droplet with 70% petrolatum content and finally stabilizes as a disk-shaped rolled form.

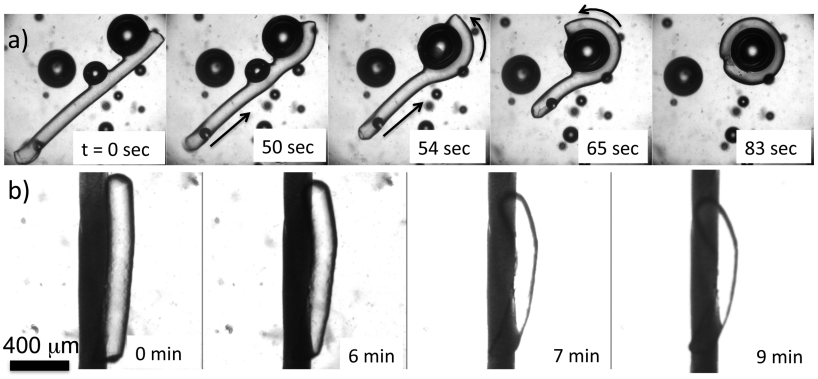

Figure 10. Biasing or guiding the direction of collapse forms additional shapes. For example, in (a), by wrapping around an attached bubble a rod can be arrested into a circular structure. Enhanced retention on surfaces, where attachment has already occurred, can be brought about by collapse as the rod in (b) is seen to wrap helically around the fiber and provide contact complexity during deposition.

wide range of complex shapes depending on the trigger, boundary conditions, and interactions with an external substrate. The reinforced grip of a droplet on a substrate could resist wash-off given the appropriately timed trigger, such as delivery to a tissue surface at biological temperature. Collapse temperatures can be tuned by choice of appropriate solids content and drop radius to match physiological temperatures or other constraints.

■ CONCLUSIONS

Although anisotropic shapes are known to be desirable for enhanced delivery of active ingredients in various formulations, the benefits of shape have previously been relevant only to solid particle systems. This work has demonstrated an approach for making shaped droplets with the potential to enhance delivery and exploit some of the benefits of shaped colloids. Shaped droplets can be produced via the extrusion of viscoelastic dispersions with a yield stress that offsets the interfacial pressure exerted on the droplet. Yield stress can be tuned by adjustment of droplet solids content, complementing the ability to control interfacial pressure by surfactant addition,[28] or adjustment of the droplet end-cap radius. A physical model of the relevant force balance[28] enables design of shaped droplets with stability against particular solution composition and temperature, allowing control of shape change by melting-induced collapse of the endoskeleton structure. Temperature-controlled collapse can also be used to transform rod-shaped droplets into more complex and compact shapes by arresting their collapse before completion. Collapse also improves drop−substrate contact during deposition onto targeted surfaces, possibly improving drop delivery and retention. The work demonstrates that endoskeleton droplets are a viable path to controlled shape and size in emulsions, with potential applications in a range of practical formulations.

■ AUTHOR INFORMATION

Corresponding Author

*E-mail: p.spicer@unsw.edu.au (P.T.S.).

Notes

The authors declare no competing financial interest.

■ ACKNOWLEDGMENTS

We gratefully acknowledge conversations with Todd Squires (UCSB) on the collapse of rod-shaped droplets.

■ REFERENCES

(1) Adamczyk, Z. Particle Transfer and Deposition from Flowing Colloid Suspensions. *Colloids Surf.* **1989**, *35*, 283−308.
(2) Champion, J.; Mitragotri, S. Role of target geometry in phagocytosis. *Proc. Natl. Acad. Sci. U. S. A.* **2006**, *103*, 4930.
(3) Adi, S.; Adi, H.; Tang, P.; Traini, D.; Chan, H.-K.; Young, P. M. Micro-particle corrugation, adhesion and inhalation aerosol efficiency. *Eur. J. Pharm. Sci.* **2008**, *35*, 12−18.
(4) Edwards, D. A.; Hanes, J.; Caponetti, G.; Hrkach, J. Large porous particles for pulmonary drug delivery. *Science* **1997**, *276*, 1868.

DOI: 10.1021/acs.langmuir.5b00321
Langmuir 2015, 31, 8558−8565

(5) Martin, A. R.; Finlay, W. H. Enhanced deposition of high aspect ratio aerosols in small airway bifurcations using magnetic field alignment. *J. Aerosol Sci.* **2008**, *39*, 679−690.
(6) Garcia, A.; Mack, P.; Williams, S.; Fromen, C.; Shen, T.; Tully, J.; Pillai, J.; Kuehl, P.; Napier, M.; DeSimone, J. Microfabricated Engineered Particle Systems for Respiratory Drug Delivery and Other Pharmaceutical Applications. *J. Drug Delivery* **2012**, *2012*, 1−10.
(7) Weiss, T.; Mills, A.; Hornberger, G.; Herman, J. Effect of Bacterial Cell Shape on Transport of Bacteria in Porous Media. *Environ. Sci. Technol.* **1995**, *29*, 1737−1740.
(8) Uspal, W. E.; Burak Eral, H.; Doyle, P. S. Engineering particle trajectories in microfluidic flows using particle shape. *Nat. Commun.* **2013**, *4*, 1−9.
(9) Sacanna, S.; Irvine, W.; Chaikin, P.; Pine, D. Lock and key colloids. *Nature* **2010**, *464*, 575−578.
(10) Dendukuri, D.; Pregibon, D.; Collins, J.; Hatton, T.; Doyle, P. Continuous-flow lithography for high-throughput microparticle synthesis. *Nat. Mater.* **2006**, *5*, 365−369.
(11) Shah, R.; Shum, H.; Rowat, A.; Lee, D.; Agresti, J.; Utada, A.; Chu, L.; Kim, J.; Fernandez-Nieves, A.; Martinez, C.; Weitz, D. Designer emulsions using microfluidics. *Mater. Today* **2008**, *11*, 18−27.
(12) Kim, J.; Vanapalli, S. A. Microfluidic Production of Spherical and Nonspherical Fat Particles by Thermal Quenching of Crystallizable Oils. *Langmuir* **2013**, *29*, 12307−12316.
(13) Subramaniam, A. B.; Abkarian, M.; Mahadevan, L.; Stone, H. Non-spherical bubbles. *Nature* **2005**, *438*, 930.
(14) Leal-Calderon, F.; Thivilliers, F.; Schmitt, V. Structured emulsions. *Curr. Opin. Colloid Interface Sci.* **2007**, *12*, 206−212.
(15) Leal-Calderon, F.; Schmitt, V. Solid-stabilized emulsions. *Curr. Opin. Colloid Interface Sci.* **2008**, *13*, 217−227.
(16) Martin, J. D.; Velankar, S. S. Unusual behavior of PEG/PPG/Pluronic interfaces studied by a spinning drop tensiometer. *J. Colloid Interface Sci.* **2008**, *322*, 669−674.
(17) Cheng, H.-L.; Velankar, S. S. Controlled jamming of particle-laden interfaces using a spinning drop tensiometer. *Langmuir* **2009**, *25*, 4412−4420.
(18) Pawar, A.; Caggioni, M.; Ergun, R.; Hartel, R.; Spicer, P. Arrested coalescence in Pickering emulsions. *Soft Matter* **2011**, *7*, 7710.
(19) Cui, M.; Emrick, T.; Russell, T. P. Stabilizing Liquid Drops in Nonequilibrium Shapes by the Interfacial Jamming of Nanoparticles. *Science* **2013**, *342*, 460−463.
(20) Raut, J. S.; Stoyanov, S. D.; Duggal, C.; Pelan, E. G.; Arnaudov, L. N.; Naik, V. M. Hydrodynamic cavitation: a bottom-up approach to liquid aeration. *Soft Matter* **2012**, *8*, 4562.
(21) Gau, H.; Herminghaus, S.; Lenz, P.; Lipowsky, R. Liquid Morphologies on Structured Surfaces: From Microchannels to Microchips. *Science* **1999**, *283*, 46.
(22) Dupuis, A.; Léopoldès, J.; Bucknall, D. G.; Yeomans, J. M. Control of drop positioning using chemical patterning. *Appl. Phys. Lett.* **2005**, *87*, 024103.
(23) Kooij, E. S.; Jansen, H. P.; Bliznyuk, O.; Poelsema, B.; Zandvliet, H. J. W. Directional wetting on chemically patterned substrates. *Colloids Surf., A* **2012**, *413*, 328−333.
(24) Ward, A.; Berry, M.; Mellor, C.; Bain, C. Optical sculpture: controlled deformation of emulsion droplets with ultralow interfacial tensions using optical tweezers. *Chem. Commun.* **2006**, *4515*, 4515.
(25) Zerrouki, D.; Rotenberg, B.; Abramson, S.; Baudry, J.; Goubault, C.; Leal-Calderon, F.; Pine, D. J.; Bibette, J. Preparation of Doublet, Triangular, and Tetrahedral Colloidal Clusters by Controlled Emulsification. *Langmuir* **2006**, *22*, 57−62.
(26) Boode, K.; Walstra, P. Partial coalescence in oil-in-water emulsions 1. Nature of the aggregation. *Colloids Surf., A* **1993**, *81*, 121−137.
(27) Pawar, A.; Caggioni, M.; Hartel, R.; Spicer, P. Arrested coalescence of viscoelastic droplets with internal microstructure. *Faraday Discuss.* **2012**, *158*, 341−350.
(28) Caggioni, M.; Bayles, A. V.; Lenis, J.; Furst, E. M.; Spicer, P. T. Interfacial stability and shape change of anisotropic endoskeleton droplets. *Soft Matter* **2014**, *10*, 7647−7652.
(29) Spicer, P.; Hartel, R. Crystal comets: Dewetting during emulsion droplet crystallization. *Aust. J. Chem.* **2005**, *58*, 655.
(30) Tjahjadi, M.; Ottino, J.; Stone, H. Estimating interfacial tension via relaxation of drop shapes and filament breakup. *AIChE J.* **1994**, *40*, 385−394.

DOI: 10.1021/acs.langmuir.5b00321
Langmuir 2015, 31, 8558−8565